RLIP76 decreases apoptosis through *Akt/mTOR* signaling pathway in gastric cancer

WENWEN WANG[1], JUAN LIU[1], JIANNI QI[2], JUNYONG ZHANG[1], QIANG ZHU[1] and CHENGYONG QIN[1]

[1]Department of Gastroenterology and [2]Central Laboratory, Shandong Provincial Hospital Affiliated to Shandong University, Jinan, Shandong 250021, P.R. China

Abstract. RLIP76 is a stress-responsive multifunctional protein and is usually overexpressed in malignant carcinomas. It plays a significant role in multiple cellular biological behaviors, including cell growth, motility, division and apoptosis, in many types of malignant cells. However, functions of RLIP76 in gastric cancer (GC) remain unknown. In the present study, RLIP76 was overexpressed in GC tissues by immunohistochemistry. RLIP76-targeted shRNA-containing lentivirus (KD) and the scrambled shRNA (NC) were used to explore the knockout of RLIP76 on cellular functions of human GC SGC-7901 and MGC-803 cells. Quantitative RT-PCR and western blotting were used to confirm that the RLIP76 was suppressed both on mRNA and protein levels after transfection. The mRNA level in SGC-7901 and MGC-803 after transfection of RLIP76-targeted shRNA was 0.245722 ± 0.021077 ($p < 0.05$) and 0.225389 ± 0.00974 ($p < 0.05$), respectively. Our results showed that the konckdown of RLIP76 downregulated cell growth after 24 h in Cell Counting Kit-8 (CCK-8) assay, reduced migration from 486.7 ± 128.8 to 219.7 ± 43.6 in SGC-7901 ($p < 0.05$) and from 630 ± 95 to 333.7 ± 46.5 in MGC-803 ($p < 0.05$), decreased invasion from 306 ± 33.5 to 97.7 ± 24.3 in SGC-7901 ($p < 0.05$) and from 350 ± 50.9 to 163.3 ± 87.5 in MGC-803 ($p < 0.05$). Length of vascular endothelial growth factor (VEGF)-induced tube formation also decreased from 202.8 ± 83.3 to 44.5 ± 3.69 in SGC-7901 and from 193 ± 3.5 to 71.8 ± 8.83 in MGC-803 ($p < 0.05$). Phosphorylation level of *Akt* declined from 138.45 ± 13.8 to $69.9 \pm 29.7\%$ in SGC-7901, and from 115.5 ± 26.6 to $49.07 \pm 27\%$ in MGC-803 ($p < 0.05$) and phosphorylation level of *mTOR* also significantly decreased ($p < 0.05$). While apoptosis of GC cells increased which we verified with apoptosis proteins and staining analysis. Our data showed that RLIP76 plays a significant oncogenic role in GC and it maybe a potential target in GC treatment.

Introduction

Gastric cancer (GC) is one of the most common types of cancer worldwide. More than 70% of new cases and deaths occur in developing countries, particularly in Eastern Asia and Europe, and South America (1). In China, GC has the second highest incidence among common types of cancers (2). Although gastric carcinoma of certain patients can be resected, these patients still have a poor prognosis; their 5-year overall survival is only approximately 20-30% (3). Many patients with GC have no chance for surgery since they were already in the advanced or metastatic stage when their GC diagnosis was confirmed (4); the median survival time of these patients is often no more than one year (5). Recurrence and metastasis are the main reasons for the high mortality rate in patients with GC (6-9). Although several anticancer drugs and different surgical modalities have been presented, GC still cannot be cured, particularly in its late stages. Thus, understanding the molecular mechanisms underlying the pathogenesis of GC is important.

Ral-interacting protein of 76 kDa, also known as RalBP1 (RLIP76) is a multifunctional protein. It is a member of the Ras family. Ras is the downstream protein of many receptor proteins, including vascular endothelial growth factor (VEGF) (10) and the activation of Ras is an important part in the pathogenesis of human malignant carcinomas. Akt pathway plays an important role in signal transduction from Ras. RLIP76 has a major role in endocytosis (11,12), mitochondrial fission (13) and cell proliferation, differentiation, apoptosis and migration (14) in normal and cancer cells. It is also an important factor in the mechanisms of drug resistance since it is capable of exporting the GSH-conjugates of alkylating chemotherapy agents, such as melphalan, as well as those of non-alkylating drugs, such as doxorubicin and vinorelbine. It participates in the formation of multi-functional protein complexes, including the mitotic spindle and the receptor signaling complexes of EGF, TGF-β, insulin and clathrin-dependent endocytosis (11,15,16) and determines the rate of receptor-ligand signaling.

Many human tissues express RLIP76, including liver, heart, ovary, lungs, muscles and kidneys. However, in multiple cancers, such as melanomas and lung and ovarian carcinomas,

Correspondence to: Dr Chengyong Qin, Shandong Provincial Hospital Affiliated to Shandong University, 324 Jingwu Weiqi Road, Jinan, Shandong 250021, P.R. China
E-mail: qinchengyongdaoshi@163.com

RLIP76 is overexpressed (17-19). In mammary tumors, over-expression of RLIP76 is positively related with advanced tumor grade and negatively related with survival (20,21). Blocking RLIP76 with targeting antibodies or antisense RNA is related to increasing sensitivity to chemotherapy and radiation, and causes pronounced tumor regression in non-small cell lung and colon carcinomas (21), prostate cancer (20) and B16 melanomas (22) in mice, and leads to apoptosis in wide varieties of histologic types of cancers in cell culture including melanoma, prostate cancer, non-small-cell lung cancer, small-cell lung, ovarian and colon cancer, lymphoma and myeloid leukemia (22-29). These data suggest that therapeutic strategies that target RLIP76 may provide a broad-spectrum anti-neoplastic approach. However, functions of RLIP76 in GC remain unknown.

In the present study, we detected RLIP76 expression in GC tissues and reduced RLIP76 expression in SGC-7901 and MGC-803 cells to explore the role of RLIP76 on cell apoptosis, angiogenesis and growth *in vitro*. Results of the present studies indicate that the suppression of the RLIP76 gene by shRNA can inhibit proliferation, induce apoptosis, reduce angiogenesis, and suppress the invasiveness of GC cells. It suggests that RLIP76 may be a potential candidate for the improvement of the therapeutic outcomes of patients with GC.

Materials and methods

Cell culture. The GC cell lines SGC-7901 and MGC-803 used in the present study were obtained from the Chinese Academy of Sciences (Shanghai, China). All cell lines were cultured in RPMI-1640 medium supplemented with 10% fetal bovine serum (FBS), penicillin G (100 U/ml) and streptomycin (100 μg/ml), and were maintained in monolayer culture at 37°C in humidified air with 5% CO_2.

Detection of cell viability by CCK-8 assay. The transfected GC cells were seeded into 96-well plates (Corning Inc., Corning, New York, NY, USA) at a density of 3,000 and 5,000 cells/well for SGC-7901 and MGC-803 cells, respectively, each well contained medium supplemented with 10% FBS. The cultures were stained using a Cell Counting Kit-8 (CCK-8; Beyotime Institute of Biotechnology, Haimen, Jiangsu, China) at various time points. Briefly, 20 μl of CCK-8 solution was added to each well, and then the solution was incubated for 4 h at 37°C. Each solution was then measured by spectrophotometry at 450 nm in a Multiskan Ascent microplate reader (Thermo Fisher Scientific Oy, Fl-01620 Vantaa, Finland).

Colony formation assay. Cells (n=500) were seeded into 60-mm plates and were allowed to attach overnight. The cells were incubated for 10 days in complete medium for colony formation. The colonies formed were washed with phosphate-buffered saline (PBS), fixed with 4% hematoxylin and stained with crystal violet. The colonies were counted and compared with the controls.

Hoechst 33342 staining analysis. The transfected GC cells were seeded into 6-well plates and were incubated at 37°C. After 24 h, the cells were stained with 0.1 μg/ml Hoechst 33342

(Sigma) for 5 min and were then observed by fluorescence microscopy using the appropriate filter for blue fluorescence.

Transwell assay. Cell migration and invasion were detected by Transwell methods. In the migration assay, cells were seeded in the upper chambers in serum-free media without a Matrigel membrane. In contrast, the lower chambers were loaded with RPMI-1640 medium supplemented with 10% FBS. After 24 or 36 h respectively, the SGC-7901 or MGC-803 cells in the upper chambers that had not migrated were removed by a cotton swab. In the invasion assay, GC cells (2×10^5) were seeded in the upper chambers in serum-free media with the Matrigel (BD) membrane, whereas the lower chambers were loaded with RPMI-1640 medium supplemented with 10% FBS. After 36 or 48 h respectively, the cells in the upper chambers that had not migrated were removed by a cotton swab. Cells were fixed with 4% polyoxymethylene. The total number of cancer cells was counted after they were fixed and stained with 4% hematoxylin.

Western blotting. Cells were washed with balanced salt solution (138 mmol/l NaCl, 5 mmol/l KCl, 0.3 mmol/l KH_2PO_4, 0.3 mmol/l Na_2HPO_4, 4 mmol/l $NaHCO_3$ and 5.6 mmol/l glucose, pH 7.4). The washed cells were lysed by buffer containing 50 mM Tris-HCl, pH 7.6, 150 mM NaCl, 0.1% sodium dodecylsulfate, 1% Nonidet P-40 and 0.5% sodium-deoxycholate, 0.1 mmol/l phenylmethylsulfonyl fluoride (PMSF) and protease inhibitor. The lysates were cooled with ice for 30 min, and then centrifuged at 4°C at 12,000 x g for 30 min. Proteins in the collected supernatant were separated by SDS-PAGE on 10 or 8% gels, and then transferred to poly-vinylidene fluoride (PVDF) membranes. The membrane, after a block with 10% skim milk was incubated with antibodies to RLIP76. The detection of β-actin (1:10,000; Santa Cruz Biotechnology, Santa Cruz, CA, USA) on the same membrane was used as the loading control. Specific antibodies for RLIP76 (ab133549, monoclonal, 1/10,000-1/50,000; Abcam, Cambridge, UK), caspase-3 (#9662, 1:1,000, polyclonal), Akt (#4691, 1:1,000, monoclonal), phosphorylated Akt (p-Akt) (#4060, 1:2,000, monoclonal), mTOR (#2983, 1:1,000, monoclonal), phosphorylated mTOR (p-mTOR) (#5536, 1:1,000, monoclonal), caspase-8 (#9746, 1:1,000, monoclonal), caspase-9 (#9508, 1:1,000, monoclonal), PARP (#9542, 1:1,000, monoclonal) (all from Cell Signaling Technology, Bedford, MA, USA) were used for the immunodetection of the corresponding proteins. HRP-conjugated secondary antibodies (1:10,000; Zhongshan Golden Bridge Biotechnology, Beijing, China), followed by enhanced chemiluminescence (Millipore Corp., Billerica, MA, USA), were used.

Patients and specimen selection. Paraffin-embedded pathological specimens were obtained from the archives of the Department of Pathology of Shandong Province Hospital Affiliated to Shandong University (P.R. China) between January 2013 and January 2014. In all, 76 samples of GC were obtained. In addition, 40 samples of normal gastric epithelial tissues that were obtained from patients who underwent surgery for gastric polyps were included in the present study. The patients were aged 28-70 years (median, 46 years). The consent procedure and study protocol were approved by the
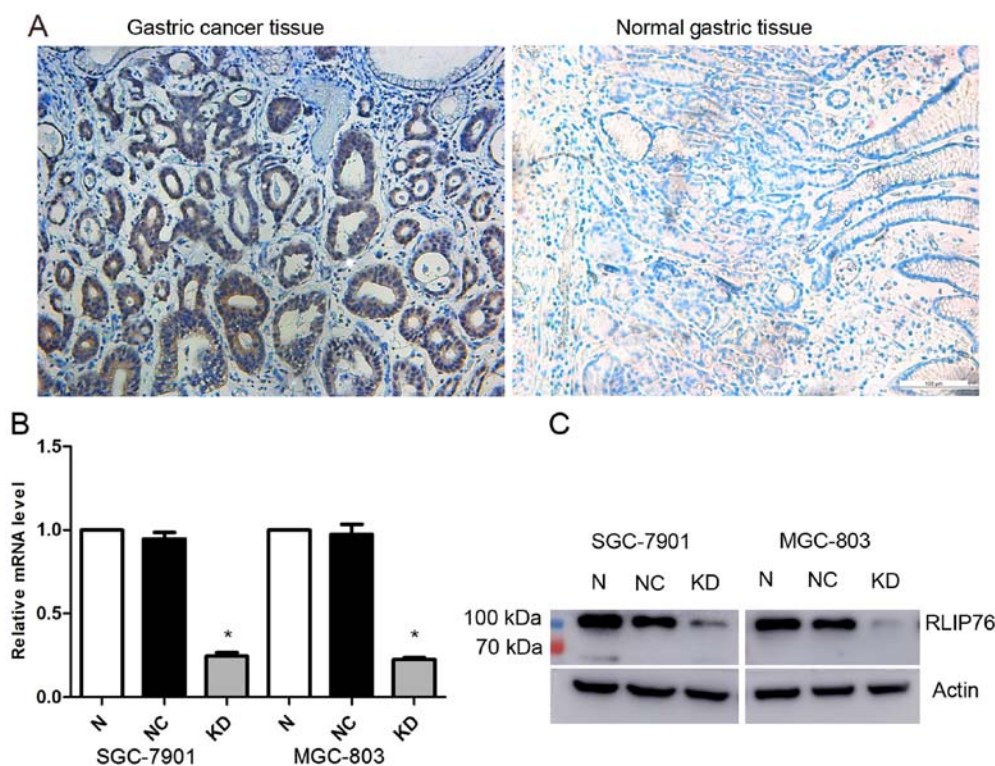
Figure 1. Levels of RLIP76 in gastric cancer and normal tissues, and the knockdown of RLIP76 in gastric cancer (GC) cells. (A) Comparison of RLIP76 levels in GC and normal gastric tissues. A higher expression level was observed in cancer tissues. (B) Quantitative RT-PCR analysis showed no significant difference of RLIP76 mRNA level between the normal and the NC cells, while the relative RLIP76 mRNA level reduced to 0.245722±0.021077 in KD SGC-7901 and 0.225389±0.00974 in KD MGC-803, respectively (*p<0.05). (C) Western blotting also demonstrated that RLIP76 was successfully knocked down in SGC-7901 and MGC-803 cells (N, represents GC cells without transfection).

Medical Ethics Committee, Shandong Provincial Hospital Affiliated to Shandong University.

Lentiviral transfection and stable cell line selection. Lentivirus that encoded RLIP76-specific shRNA and the scrambled shRNA lentivirus were supplied by GenomeDitech Co. (Shanghai, China). GC cells (SGC-7901 and MGC-803) were infected with recombinant shRNA that was specific for RLIP76 lentiviral stocks or scrambled shRNA lentiviral stocks, and stable cell clones were selected after puromycin selection. Western blotting and qRT-PCR were used to select RLIP76 knockdown cell lines (KD) and control cell lines (NC). The lentiviral vector green fluorescent protein (GFP) expressed in lentiviral vectors allowed for the assessment of the infection efficiency.

Quantitative RT-PCR analysis. Total cellular RNA was isolated with TRIzol reagent and was reverse transcribed to cDNA by M-MLV reverse transcriptase (both from Takara, Otsu, Japan) according to the manufacturer's protocol. qPCR products were detected with SYBR-Green in a LightCycler® 480 Real-Time PCR system (Roche Diagnostics, Indianapolis, IN, USA). The β-actin gene was amplified as an internal normalization. The following primers for RLIP76 were used: 5'-ggCA TgAAgTgTgAAggCATCTAC-3' and 5'-CTCgCAAATACTgC TTCAgCAAAC-3'.

Immunohistochemistry. RLIP76 protein expression was evaluated by the streptavidin-peroxidase immunohistochemical

method. Paraffin-embedded surgical specimens were sequentially cut into 4-μm thick sections. Then, the sections were deparaffinized and antigen retrieval was performed. Next, the sections were incubated with hydrogen peroxide. Mouse monoclonal antibodies to RLIP76 (ab56815, monoclonal; Abcam) were used at a dilution of 1:250 and incubated at 4°C overnight. PBS was used instead of the primary antibody, which served as a negative control. Further experimental steps were performed according to the instructions of the secondary biotinylated antibody kit purchased from ZSGB Biotech (Beijing, China).

Enzyme-linked immunosorbent assay. The transfected GC cells were seeded into 12-well plates (2x10^5) and incubated at 37°C for 24 h. Then, the culture medium was collected from the NC and KD cells. The medium was then tested by ELISA to measure the level of VEGF protein, which was performed according to the manufacturer's protocol.

Tube formation assay. Matrigel was thawed at 4°C overnight before the experiment. A 96-well plate was coated with cold Matrigel and incubated for 1 h at 37°C. Cell cultures were collected from GC cells, and mixed with HUVEC, respectively. The mixture was added to the wells and was incubated at 37°C with 5% CO$_2$. The cells were monitored every 2 h under a microscope for 6-12 h, and tube formation was imaged at 8 h.

Statistical analysis. All data were evaluated with a two-tailed unpaired Student's t-test or with a two-tailed paired Student's
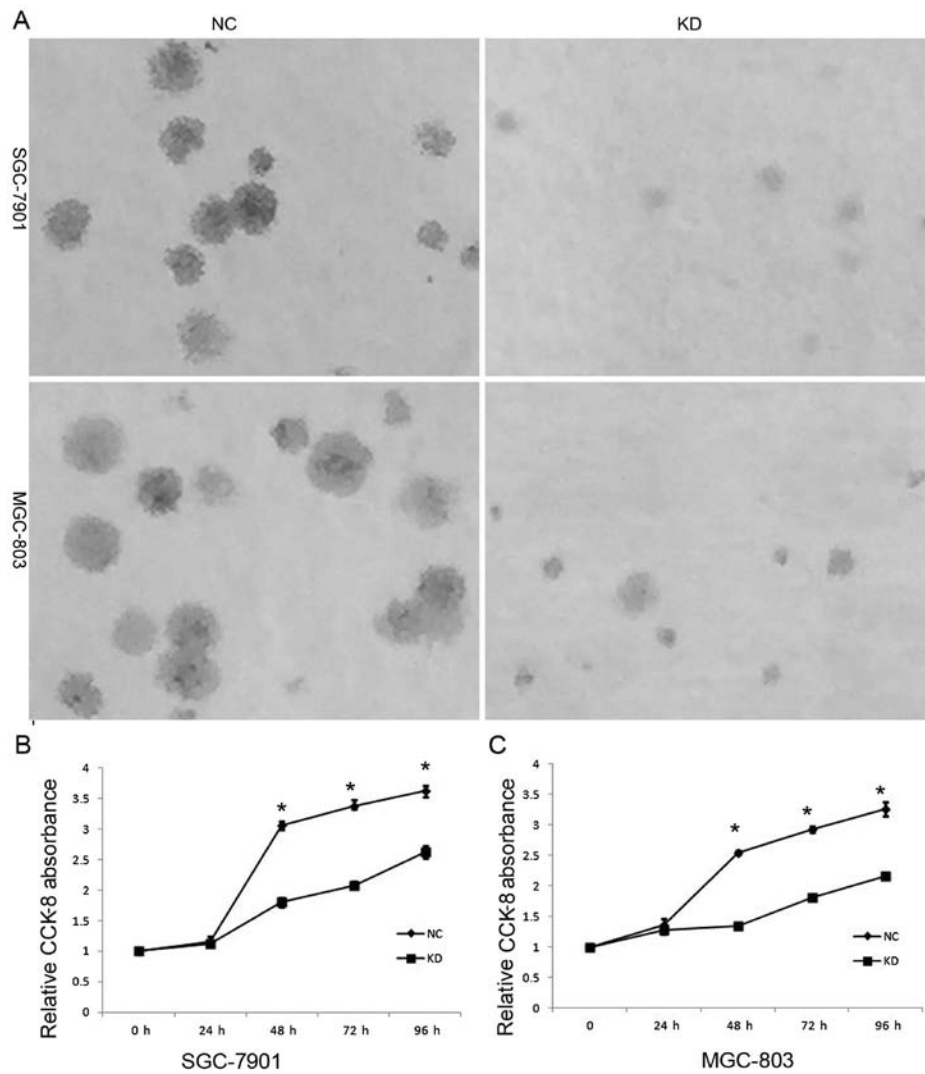
Figure 2. Effects of RLIP76 knockdown on cell growth. (A) Both KD SGC-7901 and MGC-803 cells demonstrated a significant decrease in colony formation rate. (B) The KD SGC-7901 cells exhibited significant decrease of growth compared with the control cells, particularly at the 48 h time point (*p<0.05). (C) The KD MGC-803 cells also exhibited significant inhibition of cell growth (*p<0.05).

t-test. A p-value <0.05 was considered to indicate a statistically significant result.

Results

RLIP76 is overexpressed in GC. To examine RLIP76 expression in the GC tissues included in the present study, we performed an immunohistochemical analysis. In total, 76 samples were collected and incubated with anti-RLIP76 IgG antibody. The results indicate relatively higher expression of RLIP76 in tumor tissues than in normal tissues (Fig. 1A).

shRNA decreases the RLIP76 expression in human GC SGC-7901 and MGC-803 cell lines. To evaluate the effect of the knockdown of RLIP76 on the biological behavior of GC cell lines, RNA interference vectors: lentivirus encoding shRNA specific for RLIP76 (KD) and the control (NC), were designed for specific interference of the endogenous RLIP76 gene. RLIP76 expression was detected by qRT-PCR and western blot analysis. As shown in Fig. 1B, no significant difference of RLIP76 mRNA level was found between the normal and

the NC cells, but a significantly lower level of RLIP76 mRNA expression in KD cells (p<0.05). The relative RLIP76 mRNA level reduced to 0.245722±0.021077 in KD SGC-7901 and 0.225389±0.00974 in KD MGC-803, respectively. Western blot analysis also displayed a significant reduction in RLIP76 expression in both transfected cell lines (Fig. 1B).

Knockdown of RLIP76 decreases cell proliferation and increases apoptosis of GC cells through Akt/mTOR signaling pathway. To investigate the biological function of RLIP76 in the development and progression of GC, we performed a colony formation and a CCK-8 assay after transfection of GC cells. The SGC-7901 and MGC-803 cells that were transfected with RLIP76 shRNA formed fewer and smaller colonies than the NC cells (Fig. 2A). As shown in Fig. 2B and C, the KD GC cells displayed significant growth decrease compared with the NC cells after 24 h, including 48, 72 and 96 h (p<0.05).

Apoptosis is one of the predominant types of programmed cell death that involves a series of biochemical events that lead to specific cell morphological changes, including cell shrinkage, nuclear fragmentation, chromatin condensation and
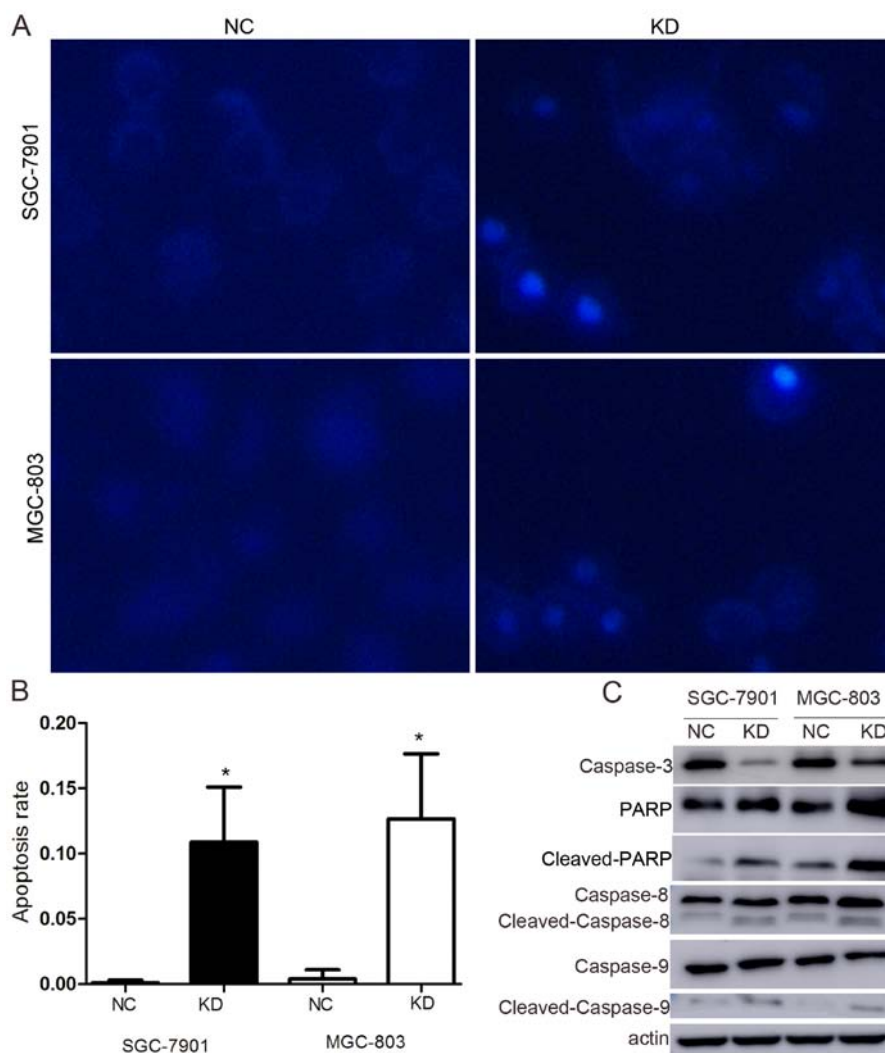
Figure 3. Apoptosis increases after shRNA transfection. (A) Hoechst staining showed increased number of apoptotic cells in the KD versions of both cell lines (*p<0.05). (B) The apoptosis rate increased from 0.11±0.18 to 10.87±4.2% in SGC-7901 and from 0.40±0.69 to 12.67±4.98% in MGC-803 (*p<0.05). (C) The level of caspase-3 in both KD SGC-7901 and MGC-803 cell lines was markedly decreased when compared with the controls, whereas the levels of cleaved-PARP, cleaved-caspase-8 and cleaved-caspase-9 increased.

chromosomal DNA fragmentation. As shown in Fig. 3A and B, the degrees of nuclear fragmentation and chromatin condensation were greater in the KD cells than in the NC cells in both cell lines. The apoptosis rate increased from 0.11±0.18 to 10.87±4.2% in SGC-7901 and from 0.40±0.69 to 12.67±4.98% in MGC-803 (p<0.05).

To confirm the influence of RLIP76 knockdown relative to apoptosis in GC cells, the expression of apoptosis-associated proteins, such as caspase-3, PARP, caspase-8 and -9, were detected by western blotting. The results showed that caspase-3 expression decreased, whereas cleaved PARP, cleaved-caspase-8 and cleaved-caspase-9 were significantly increased (Fig. 3C).

In contrast, in order to identify which signaling pathway was associated with apoptosis, we analyzed the levels of *Akt* and *mTOR* and their phosphorylation levels in the transfected GC cells by western blot analysis (Fig. 4A). The knockdown of RLIP76 significantly reduced phosphorylation of *Akt* [from 138.45±13.8 to 69.9±29.7% in SGC-7901 (p<0.05), and from 115.5±26.6 to 49.07±27% in MGC-803 (p<0.05)] (Fig. 4B) and *mTOR* in both GC cell lines significantly (Fig. 4C)

(p<0.05). The activation suppression of *p-Akt* leads to further suppression of *mTOR*, which suppresses the expression of pro-apoptotic Bim and favors the survival and proliferation of cancer cells (30).

Knockdown of RLIP76 decreases migration and invasion of GC cells. To assess the effect of RLIP76 knockdown on SGC-7901 and MGC-803 cell lines with respect to migration and invasion, we performed an *in vitro* migration and invasion assay using NC and KD GC cells. A decrease in cell migration and invasion was observed in KD cells (Fig. 5), which suggests that RLIP76 knockdown significantly suppressed invasion and migration of GC cells *in vitro* (in migration assay, SGC-7901, NC 486.7±128.8, KD 219.7±43.6; MGC-803, NC 630±95, KD 333.7±46.5; in invasion assay, SGC-7901, NC 306±33.5, KD 97.7±24.3; MGC-803, NC 350±50.9, KD 163.3±87.5) (p<0.05).

Knockdown of RLIP76 downregulates VEGF secretion in GC cells. We observed that knockdown of RLIP76 reduced VEGF section from 465±2.12 to 158.6 ±6.93 in SGC-7901 and
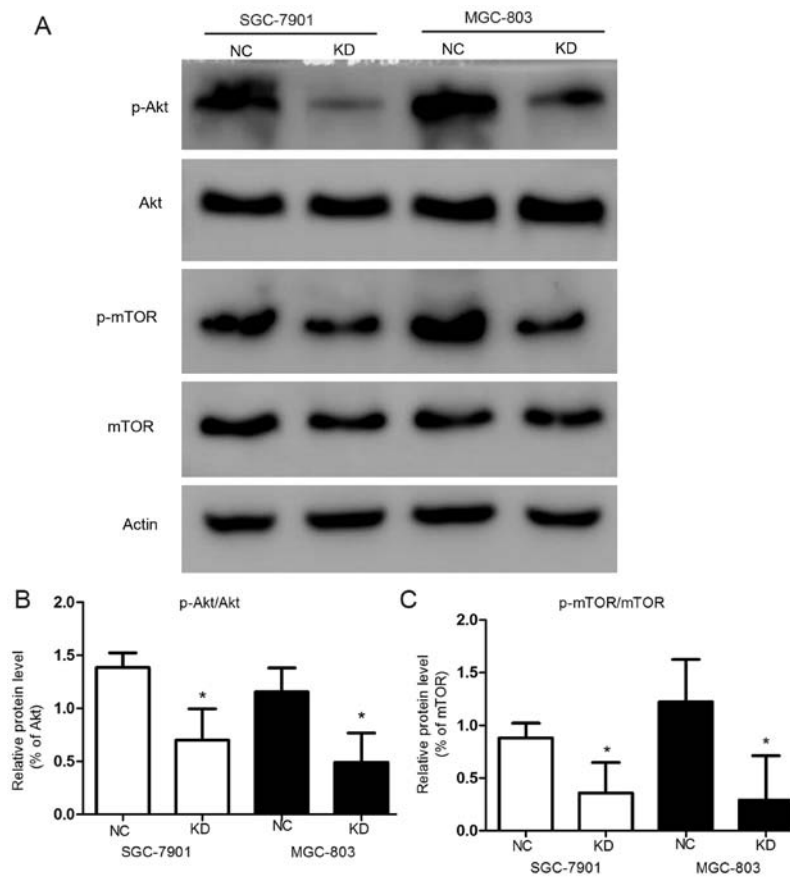
Figure 4. Knockdown of RLIP76 causes different phosphorylation levels of *Akt* and *mTOR*. In KD cells, the levels of phosphorylated *Akt* (*p-Akt*) decreased from 138.45±13.8 to 69.9±29.7% in SGC-7901, and from 115.5±26.6 to 49.07±27% in MGC-803 (*p<0.05) and phosphorylated *mTOR* (*p-mTOR*) level also decreased, whereas the levels of *Akt* and *mTOR* remained the same.
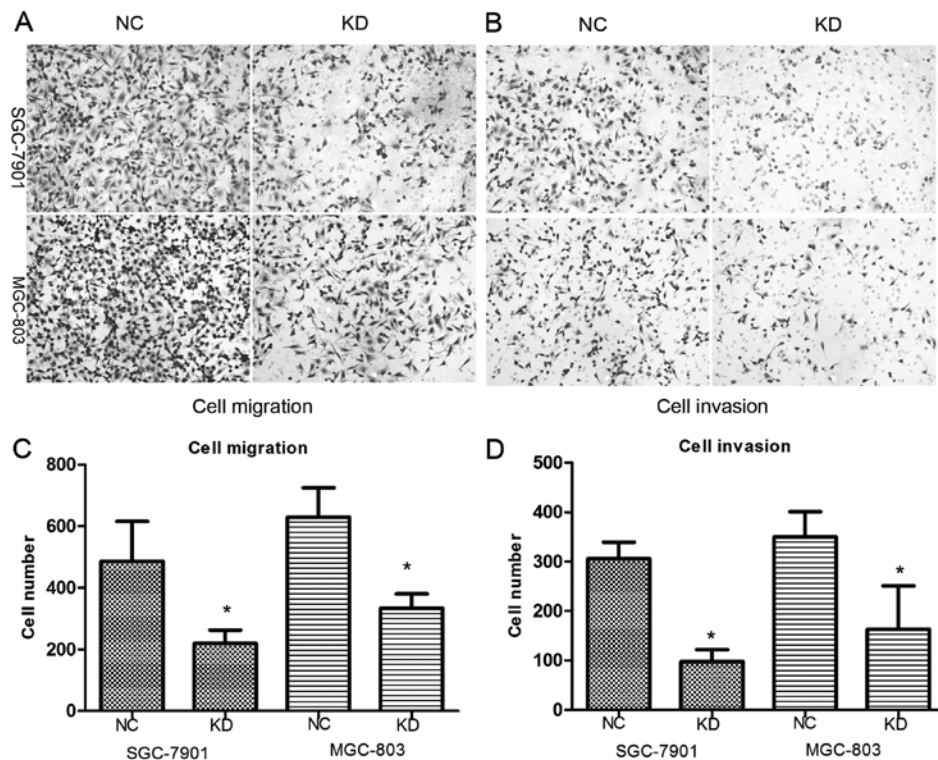

Figure 5. (A-D) Migration and invasion were decreased after shRNA transfection. The number of cells that migrated across the membrane with or without cold Matrigel demonstrated that fewer KD cells can migrate compared with control cells. In migration assay, SGC-7901, NC 486.7±128.8, KD 219.7±43.6; MGC-803, NC 630±95, KD 333.7±46.5 (*p<0.05). In invasion assay, SGC-7901, NC 306±33.5, KD 97.7±24.3; MGC-803, NC 350±50.9, KD 163.3±87.5) (*p<0.05).
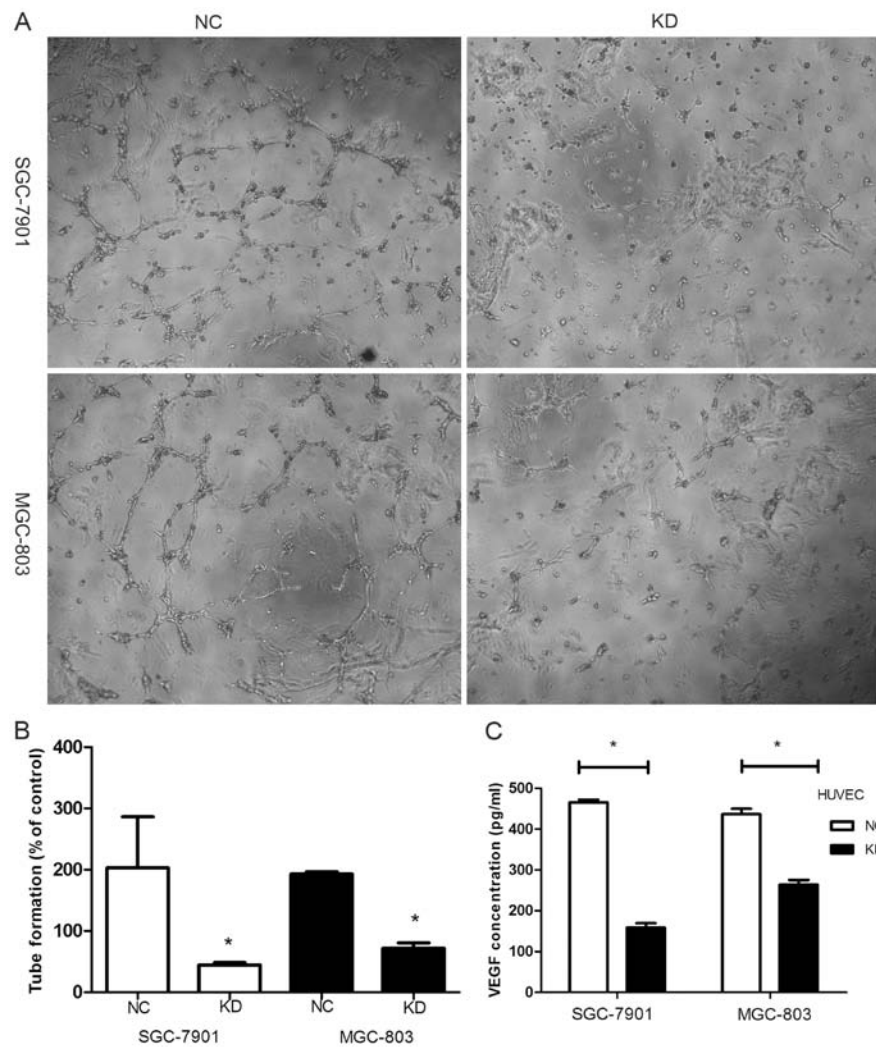
Figure 6. Relationship between RLIP76 and VEGF. (A and B) Fewer tubes formed in the KD cells. The relative length of tube decreased from 202.8±83.3 to 44.5±3.69 in SGC-7901 (*p<0.05) and from 193±3.5 to 71.8±8.83 in MGC-803 (*p<0.05) (% of control). (C) The level of VEGF secretion decreased from 465±2.12 to 158.6 ±6.93 in SGC-7901 and from 463.5 ±13.6 to 264 ±11.2 in MGC-803 (pg/ml) (*p<0.05).

from 463.5 ±13.6 to 264 ±11.2 in MGC-803 (pg/ml) (Fig. 6C) (p<0.05). Tube formation by endothelial cells, which serves as an *in vitro* measure of angiogenesis, was assessed after HUVEC cells were incubated with supernatant of GC cells for 8 h. Photomicrographs of cells showed that tube formation was inhibited more strongly in the KD cell lines (Fig. 6A). The average tube length in supernatant of the KD cells was markedly shorter than that in the NC cells (% of control) (Fig. 6B) [SGC-7901 NC, 202.8±83.3; KD, 44.5±3.69 (p<0.05); MGC-803 NC, 193±3.5; KD, 71.8±8.83 (p<0.05)].

Discussion

RLIP76 is overexpressed in a variety of solid tumors, such as kidney and prostate cancer, among others. The proposed mechanism of action for RLIP76-targeted therapy is completely different from most current approaches, which mainly concentrate on chemicals that modify kinases or phosphatases (31). In the present study, we determined that the expression and specific activity of the RLIP76 protein are relatively higher in gastric cancer (GC) tissues than in normal tissues. The present study was designed to elucidate the functional role and regulation of critical pro-survival signaling pathways of RLIP76 in the biological activities of GC cells. shRNA was used to suppress the RLIP76 expression and the connections between RLIP76 and proliferation, apoptosis, cellular migration, invasion and VEGF secretion were investigated. A significant finding of the present study is that the knockdown of RLIP76 effectively suppresses the level of *Akt* phosphorylation, decreases the expression of *p-mTOR*, and activates a sequence of apoptotic signaling proteins. This may provide a collective rationale for the effective regulation of the *Akt/mTOR* pathway and the activation of apoptosis following RLIP76 depletion.

In the present study, we found that the downregulation of RLIP76 expression reduces the proliferation of GC cells while increasing apoptosis, which is consistent with previous studies. We performed colony formation assay and measured the expression levels of caspase-3, -8 and -9 and PARP1 proteins. The knockdown of RLIP76 decreased colony formation and increased the expression of cleaved-caspase-3, cleaved-caspase-8, cleaved-caspase-9 and cleaved-PARP at the protein level, which implies a functional interaction between RLIP76 and caspase pathways in GC. These data

strongly support the conclusion that one of the physiological functions of RLIP76 is to downregulate apoptotic signaling. This process possibly occurs via the control of intracellular levels of pro-apoptotic endogenous lipid-peroxidation byproducts, followed by the catalysis of the efflux of GS-E. 4HNE (and other alkenals) alone triggers apoptosis (32-39), and the inhibition of RLIP76 has been shown to increase the intracellular accumulation of 4HNE (40,41). However, other potential RLIP76-mediated mechanisms for the inhibition of apoptosis remain unclear. As RLIP76 is a member of Ras family, *Akt* pathway may play an important role in signal transduction. The present study showed a significant relationship between the *Akt/mTOR* signaling pathway and RLIP76. The decreased expression of p-*Akt* and *p-mTOR* after RLIP76 knockdown demonstrates that RLIP76 plays a vital role in regulating GC cell apoptosis. RLIP76 has also been shown to exhibit GAP activity toward cdc42. Activation of the Rho family G-protein, cdc42, has been shown to induce apoptosis (42). It has been reported that overexpression of POB1, which is the partner of RLIP76 triggers apoptosis in prostate cancer cells (43). POB1 has been demonstrated to be a specific inhibitor of the transport of DOX and GS-E by RLIP76. The fact that the augmentation of POB1 also triggers apoptosis in the absence of any chemotherapy drug in lung cancer cells has been established. The inhibition of cellular RLIP76 via an increase in POB1 also results in the increased accumulation and decreased efflux of DOX, as well as significant sensitization to DOX (44).

RLIP76 deletion in mice inhibiting angiogenesis in xenografted tumors has been demonstrated. As Ras is the downstream protein of VEGF, the relationship between RLIP76 and VEGF was explored. In the present study, RLIP76 suppression decreased VEGF section and VEGF-induced tube formation *in vitro*. Since VEGF is important in tumor cells, such as regulating receptor surface expression, it could influence the tumor cell function (45). *PI3K* has been shown involved in VEGF secretion in many cells, and may be a major regulator of VEGF secretion in angiogenic environments (46-49). However, the mechanisms by which RLIP76 regulates VEGF secretion remain to be explored.

In conclusion, the present study shows that RLIP76 is overexpressed in GC tissues and knockdown of RLIP76 in GC cells significantly suppresses growth, decreases VEGF section and tube formation, and increases apoptosis through *Akt/mTOR* signaling pathway. Although further studies are needed, results of the present study suggest that RLIP76 may be a potential therapy target for GC treatment and may be used with conventional therapeutics to increase treatment efficacy.

Acknowledgements

References

1. Jemal A, Bray F, Center MM, Ferlay J, Ward E and Forman D: Global cancer statistics. CA Cancer J Clin 61: 69-90, 2011.
2. Chen W, Zheng R, Zhang S, Zhao P, Zeng H, Zou X and He J: Annual report on status of cancer in China, 2010. Chin J Cancer Res 26: 48-58, 2014.
3. Quéro L, Guillerm S and Hennequin C: Neoadjuvant or adjuvant therapy for gastric cancer. World J Gastrointest Oncol 7: 102-110, 2015.
4. Dassen AE, Lemmens VE, van de Poll-Franse LV, Creemers GJ, Brenninkmeijer SJ, Lips DJ, Vd Wurff AA, Bosscha K and Coebergh JW: Trends in incidence, treatment and survival of gastric adenocarcinoma between 1990 and 2007: A population-based study in the Netherlands. Eur J Cancer 46: 1101-1110, 2010.
5. Oba K, Paoletti X, Bang YJ, Bleiberg H, Burzykowski T, Fuse N, Michiels S, Morita S, Ohashi Y, Pignon JP, *et al*; GASTRIC (Global Advanced/Adjuvant Stomach Tumor Research International Collaboration) Group: Role of chemotherapy for advanced/recurrent gastric cancer: An individual-patient-data meta-analysis. Eur J Cancer 49: 1565-1577, 2013.
6. Buchner AM, Shahid MW, Heckman MG, Krishna M, Ghabril M, Hasan M, Crook JE, Gomez V, Raimondo M, Woodward T, *et al*: Comparison of probe-based confocal laser endomicroscopy with virtual chromoendoscopy for classification of colon polyps. Gastroenterology 138: 834-842, 2010.
7. Li WB, Zuo XL, Li CQ, Zuo F, Gu XM, Yu T, Chu CL, Zhang TG and Li YQ: Diagnostic value of confocal laser endomicroscopy for gastric superficial cancerous lesions. Gut 60: 299-306, 2011.
8. Sanduleanu S, Driessen A, Gomez-Garcia E, Hameeteman W, de Bruïne A and Masclee A: In vivo diagnosis and classification of colorectal neoplasia by chromoendoscopy-guided confocal laser endomicroscopy. Clin Gastroenterol Hepatol 8: 371-378, 2010.
9. Wallace M, Lauwers GY, Chen Y, Dekker E, Fockens P, Sharma P and Meining A: Miami classification for probe-based confocal laser endomicroscopy. Endoscopy 43: 882-891, 2011.
10. Downward J: Targeting RAS signalling pathways in cancer therapy. Nat Rev Cancer 3: 11-22, 2003.
11. Jullien-Flores V, Mahé Y, Mirey G, Leprince C, Meunier-Bisceuil B, Sorkin A, Camonis JH, Gacon G and Camonis JH: RLIP76, an effector of the GTPase Ral, interacts with the AP2 complex: Involvement of the Ral pathway in receptor endocytosis. J Cell Sci 113: 2837-2844, 2000.
12. Nakashima S, Morinaka K, Koyama S, Ikeda M, Kishida M, Okawa K, Iwamatsu A, Kishida S and Kikuchi A: Small G protein Ral and its downstream molecules regulate endocytosis of EGF and insulin receptors. EMBO J 18: 3629-3642, 1999.
13. Kashatus DF, Lim KH, Brady DC, Pershing NL, Cox AD and Counter CM: RALA and RALBP1 regulate mitochondrial fission at mitosis. Nat Cell Biol 13: 1108-1115, 2011.
14. Goldfinger LE, Ptak C, Jeffery ED, Shabanowitz J, Hunt DF and Ginsberg MH: RLIP76 (RalBP1) is an R-Ras effector that mediates adhesion-dependent Rac activation and cell migration. J Cell Biol 174: 877-888, 2006.
15. Quaroni A and Paul EC: Cytocentrin is a Ral-binding protein involved in the assembly and function of the mitotic apparatus. J Cell Sci 112: 707-718, 1999.
16. Awasthi S, Singhal SS, Sharma R, Zimniak P and Awasthi YC: Transport of glutathione conjugates and chemotherapeutic drugs by RLIP76 (RALBP1): A novel link between G-protein and tyrosine kinase signaling and drug resistance. Int J Cancer 106: 635-646, 2003.
17. Awasthi S, Singhal SS, Awasthi YC, Martin B, Woo JH, Cunningham CC and Frankel AE: RLIP76 and cancer. Clin Cancer Res 14: 4372-4377, 2008.
18. Awasthi S, Singhal SS, Srivastava SK, Zimniak P, Bajpai KK, Saxena M, Sharma R, Ziller SA III, Frenkel EP and Singh SV: Adenosine triphosphate-dependent transport of doxorubicin, daunomycin, and vinblastine in human tissues by a mechanism distinct from the P-glycoprotein. J Clin Invest 93: 958-965, 1994.
19. Awasthi YC, Singhal SS, Gupta S, Ahmad H, Zimniak P, Radominska A, Lester R and Sharma R: Purification and characterization of an ATPase from human liver which catalyzes ATP hydrolysis in the presence of the conjugates of bilirubin bile acids and glutathione. Biochem Biophys Res Commun 175: 1090-1096, 1991.
20. Singhal SS, Roth C, Leake K, Singhal J, Yadav S and Awasthi S: Regression of prostate cancer xenografts by RLIP76 depletion. Biochem Pharmacol 77: 1074-1083, 2009.

21. Singhal SS, Singhal J, Yadav S, Dwivedi S, Boor PJ, Awasthi YC and Awasthi S: Regression of lung and colon cancer xenografts by depleting or inhibiting RLIP76 (Ral-binding protein 1). Cancer Res 67: 4382-4389, 2007.
22. Singhal SS, Awasthi YC and Awasthi S: Regression of melanoma in a murine model by RLIP76 depletion. Cancer Res 66: 2354-2360, 2006.
23. Awasthi S, Singhal SS, Singhal J, Cheng J, Zimniak P and Awasthi YC: Role of RLIP76 in lung cancer doxorubicin resistance: II. Doxorubicin transport in lung cancer by RLIP76. Int J Oncol 22: 713-720, 2003.
24. Awasthi S, Singhal SS, Singhal J, Yang Y, Zimniak P and Awasthi YC: Role of RLIP76 in lung cancer doxorubicin resistance: III. Anti-RLIP76 antibodies trigger apoptosis in lung cancer cells and synergistically increase doxorubicin cytotoxicity. Int J Oncol 22: 721-732, 2003.
25. Yadav S, Singhal SS, Singhal J, Wickramarachchi D, Knutson E, Albrecht TB, Awasthi YC and Awasthi S: Identification of membrane-anchoring domains of RLIP76 using deletion mutant analyses. Biochemistry 43: 16243-16253, 2004.
26. Stuckler D, Singhal J, Singhal SS, Yadav S, Awasthi YC and Awasthi S: RLIP76 transports vinorelbine and mediates drug resistance in non-small cell lung cancer. Cancer Res 65: 991-998, 2005.
27. Singhal SS, Yadav S, Singhal J, Zajac E, Awasthi YC and Awasthi S: Depletion of RLIP76 sensitizes lung cancer cells to doxorubicin. Biochem Pharmacol 70: 481-488, 2005.
28. Awasthi S, Cheng J, Singhal SS, Saini MK, Pandya U, Pikula S, Bandorowicz-Pikula J, Singh SV, Zimniak P and Awasthi YC: Novel function of human RLIP76: ATP-dependent transport of glutathione conjugates and doxorubicin. Biochemistry 39: 9327-9334, 2000.
29. Awasthi S, Cheng JZ, Singhal SS, Pandya U, Sharma R, Singh SV, Zimniak P and Awasthi YC: Functional reassembly of ATP-dependent xenobiotic transport by the N- and C-terminal domains of RLIP76 and identification of ATP binding sequences. Biochemistry 40: 4159-4168, 2001.
30. Sugatani T and Hruska KA: Akt1/Akt2 and mammalian target of rapamycin/Bim play critical roles in osteoclast differentiation and survival, respectively, whereas Akt is dispensable for cell survival in isolated osteoclast precursors. J Biol Chem 280: 3583-3589, 2005.
31. Singhal SS, Singhal J, Figarola J, Horne D and Awasthi S: RLIP76 targeted therapy for kidney cancer. Pharm Res 32: 3123-3136, 2015.
32. Yang Y, Sharma A, Sharma R, Patrick B, Singhal SS, Zimniak P, Awasthi S and Awasthi YC: Cells preconditioned with mild, transient UVA irradiation acquire resistance to oxidative stress and UVA-induced apoptosis: Role of 4-hydroxynonenal in UVA-mediated signaling for apoptosis. J Biol Chem 278: 41380-41388, 2003.
33. Zhang W, He Q, Chan LL, Zhou F, El Naghy M, Thompson EB and Ansari NH: Involvement of caspases in 4-hydroxy-alkenal-induced apoptosis in human leukemic cells. Free Radic Biol Med 30: 699-706, 2001.
34. Cheng JZ, Singhal SS, Saini M, Singhal J, Piper JT, Van Kuijk FJ, Zimniak P, Awasthi YC and Awasthi S: Effects of mGST A4 transfection on 4-hydroxynonenal-mediated apoptosis and differentiation of K562 human erythroleukemia cells. Arch Biochem Biophys 372: 29-36, 1999.
35. Cheng JZ, Singhal SS, Sharma A, Saini M, Yang Y, Awasthi S, Zimniak P and Awasthi YC: Transfection of mGSTA4 in HL-60 cells protects against 4-hydroxynonenal-induced apoptosis by inhibiting JNK-mediated signaling. Arch Biochem Biophys 392: 197-207, 2001.
36. Sharma R, Brown D, Awasthi S, Yang Y, Sharma A, Patrick B, Saini MK, Singh SP, Zimniak P, Singh SV, et al: Transfection with 4-hydroxynonenal-metabolizing glutathione S-transferase isozymes leads to phenotypic transformation and immortalization of adherent cells. Eur J Biochem 271: 1690-1701, 2004.
37. Camandola S, Poli G and Mattson MP: The lipid peroxidation product 4-hydroxy-2,3-nonenal increases AP-1-binding activity through caspase activation in neurons. J Neurochem 74: 159-168, 2000.
38. Soh Y, Jeong KS, Lee IJ, Bae MA, Kim YC and Song BJ: Selective activation of the c-Jun N-terminal protein kinase pathway during 4-hydroxynonenal-induced apoptosis of PC12 cells. Mol Pharmacol 58: 535-541, 2000.
39. Liu W, Kato M, Akhand AA, Hayakawa A, Suzuki H, Miyata T, Kurokawa K, Hotta Y, Ishikawa N and Nakashima I: 4-hydroxynonenal induces a cellular redox status-related activation of the caspase cascade for apoptotic cell death. J Cell Sci 113: 635-641, 2000.
40. Cheng JZ, Sharma R, Yang Y, Singhal SS, Sharma A, Saini MK, Singh SV, Zimniak P, Awasthi S and Awasthi YC: Accelerated metabolism and exclusion of 4-hydroxynonenal through induction of RLIP76 and hGST5.8 is an early adaptive response of cells to heat and oxidative stress. J Biol Chem 276: 41213-41223, 2001.
41. Awasthi YC, Yang Y, Tiwari NK, Patrick B, Sharma A, Li J and Awasthi S: Regulation of 4-hydroxynonenal-mediated signaling by glutathione S-transferases. Free Radic Biol Med 37: 607-619, 2004.
42. Su JL, Lin MT, Hong CC, Chang CC, Shiah SG, Wu CW, Chen ST, Chau YP and Kuo ML: Resveratrol induces FasL-related apoptosis through Cdc42 activation of ASK1/JNK-dependent signaling pathway in human leukemia HL-60 cells. Carcinogenesis 26: 1-10, 2005.
43. Oosterhoff JK, Penninkhof F, Brinkmann AO, Anton Grootegoed J and Blok LJ: REPS2/POB1 is downregulated during human prostate cancer progression and inhibits growth factor signalling in prostate cancer cells. Oncogene 22: 2920-2925, 2003.
44. Yadav S, Zajac E, Singhal SS, Singhal J, Drake K, Awasthi YC and Awasthi S: POB1 over-expression inhibits RLIP76-mediated transport of glutathione-conjugates, drugs and promotes apoptosis. Biochem Biophys Res Commun 328: 1003-1009, 2005.
45. Goel HL and Mercurio AM: VEGF targets the tumour cell. Nat Rev Cancer 13: 871-882, 2013.
46. Karar J and Maity A: PI3K/AKT/mTOR pathway in angiogenesis. Front Mol Neurosci 4: 51, 2011.
47. Moriya R, Takahashi K, Kitahara A, Onuma H, Handa K, Sumitani Y, Tanaka T, Katsuta H, Nishida S, Itagaki E, et al: Possible involvement of PI3K-dependent pathways in the increased VEGF120 release from osteoblastic cells preloaded with palmitate in vitro. Biochem Biophys Res Commun 445: 275-281, 2014.
48. Zhao W, Guo W, Zhou Q, Ma SN, Wang R, Qiu Y, Jin M, Duan HQ and Kong D: In vitro antimetastatic effect of phosphatidylinositol 3-kinase inhibitor ZSTK474 on prostate cancer PC3 cells. Int J Mol Sci 14: 13577-13591, 2013.
49. Takahashi K, Miyokawa-Gorin K, Handa K, Kitahara A, Moriya R, Onuma H, Sumitani Y, Tanaka T, Katsuta H, Nishida S, et al: Endogenous oxidative stress, but not ER stress, induces hypoxia-independent VEGF$_{120}$ release through PI3K-dependent pathways in 3T3-L1 adipocytes. Obesit 21: 1625-1634, 2013.